Electronic Supplementary Material (ESI) for Dalton Transactions.

Supporting Information

N, N-Dimethylformamide Protected Rhodium Nanocluster with Engrossing Optical Property and Their Application

Manju P. Maman[a], Saniya Gratious[a], Aparna R K[a] and Sukhendu Mandal*[a]

[a]School of Chemistry, Indian Institute of Science Education and Research Thiruvananthapuram, Maruthamala P. O., Vithura, Thiruvananthapuram, Kerala, India-695551.

Email: sukhendu@iisertvm.ac.in

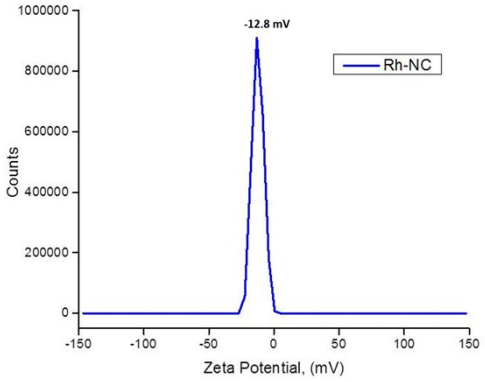

Figure S1: Surface zeta potential graph showing negative zeta potential value.

a)

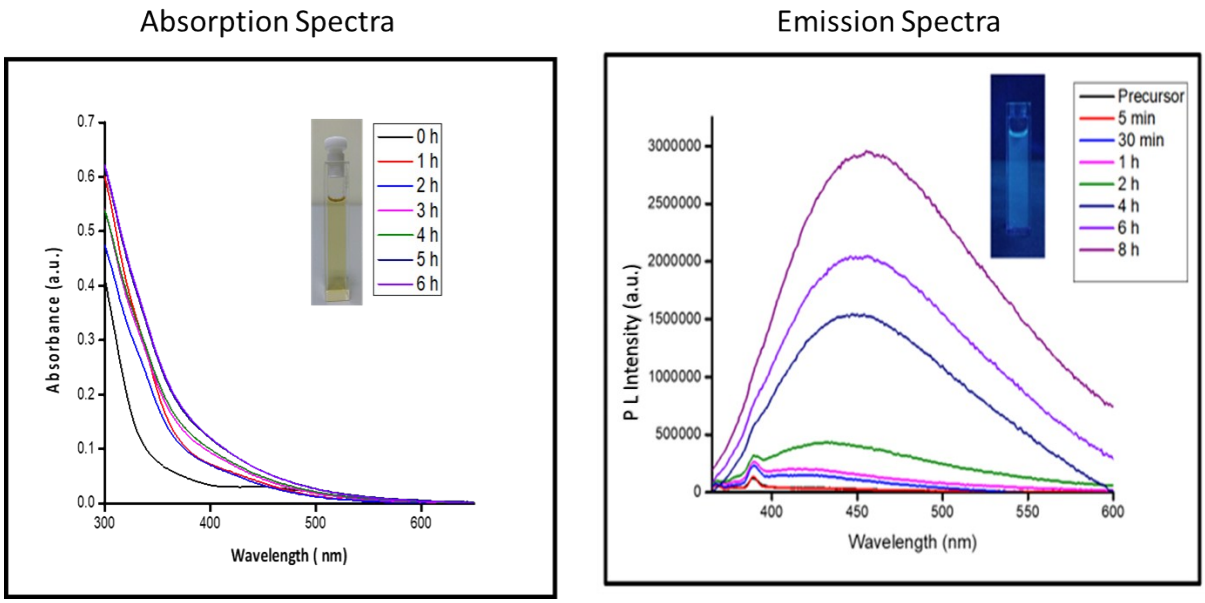

b)

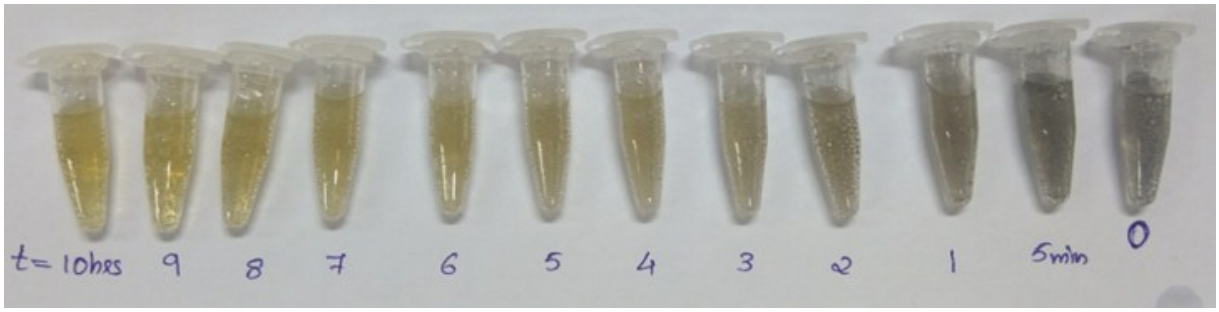

Figure S2: a) Controlled experiments (absorption and emission) to monitor the completion of Rh NC synthesis. b) Photograph of the sample after being reduced by 1 equiv. of $NaBH_4$ at different time intervals.

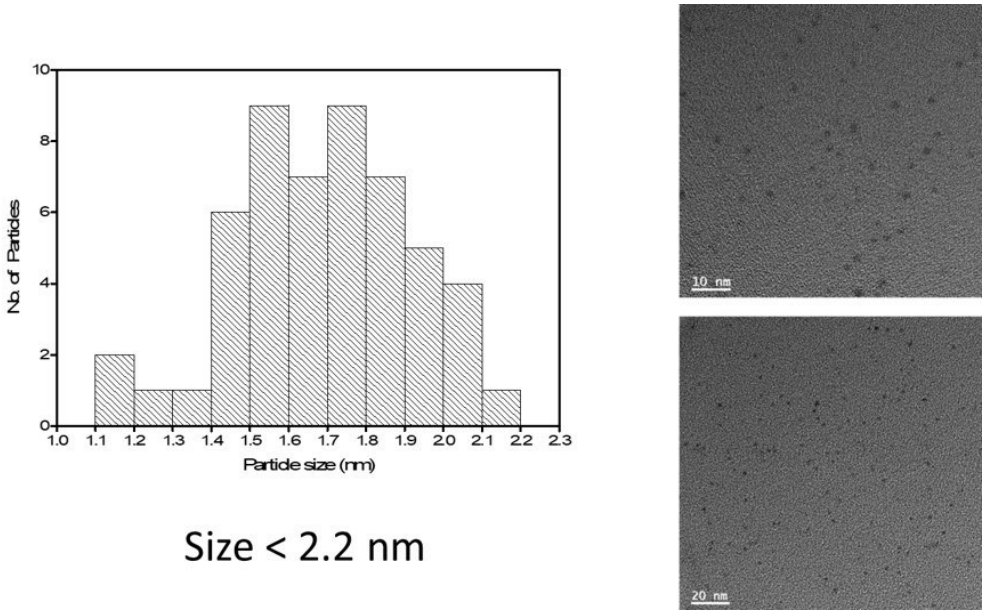

Figure S3: TEM images and bar diagram of the as-synthesized DMF protected rhodium nanocluster.

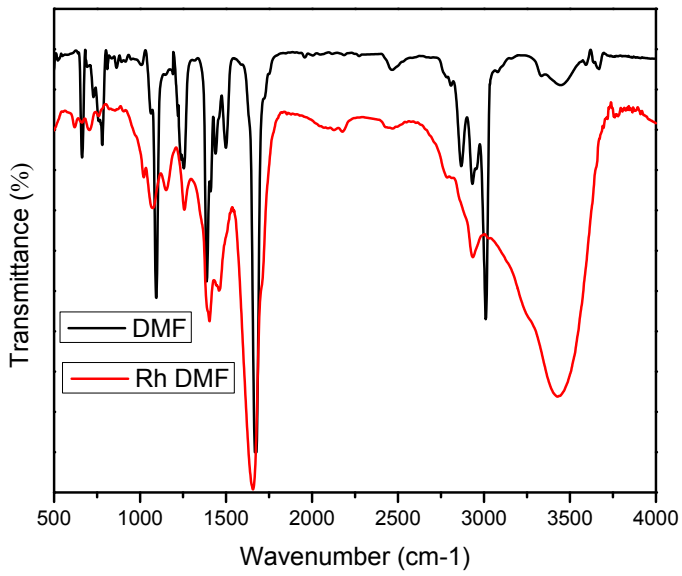
Transmittance (%)
DMF
Rh DMF
500
1000
1500
2000
2500
3000
3500
4000
Wavenumber (cm-1)

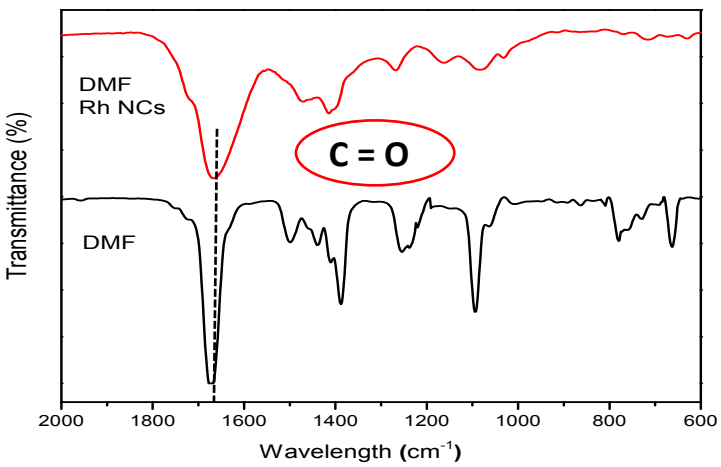
Transmittance (%)
DMF
Rh NCs
C = O
DMF
2000
1800
1600
1400
1200
1000
800
600
Wavelength (cm-1)

Figure S4: Infrared spectra of pure DMF molecule and DMF protected Rh NC. Note that boarding and shifting of C=O stretching at lower wave numbers (1673 to 1656 cm^{-1}) indicating the interaction of DMF molecules with Rh metal ion in the cluster.

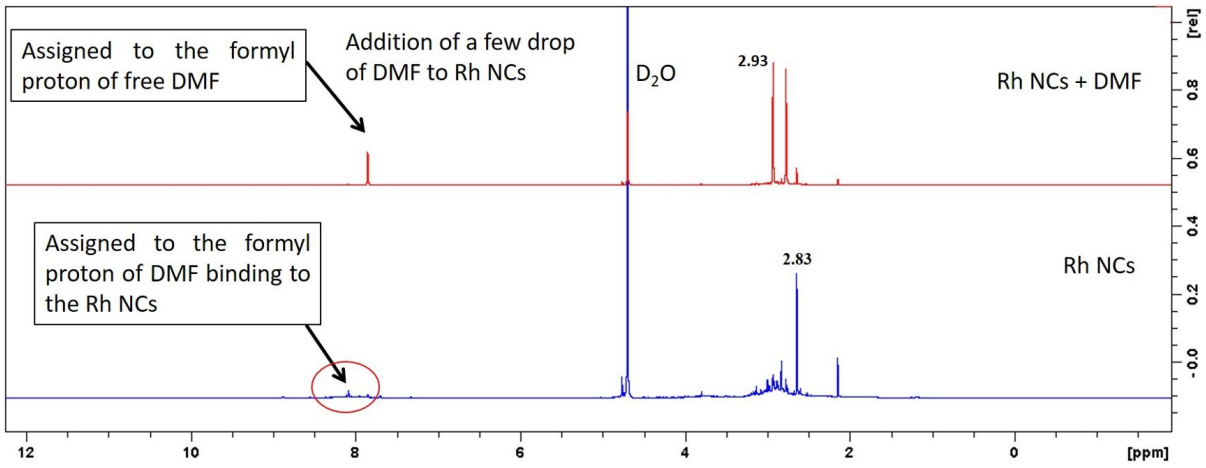

Figure S5: ^{1}H NMR spectra in D_2O for DMF bonded Rh cluster and freely added DMF into the Rh NCs.

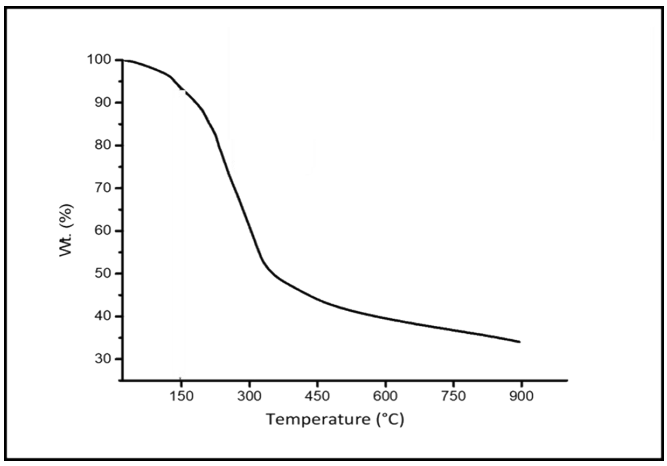
100
90
80
70
60
50
40
30
Wt. (%)
150
300
450
600
750
900
Temperature (°C)

Figure S6: Thermogravimetric plot of DMF-bonded Rh NC.

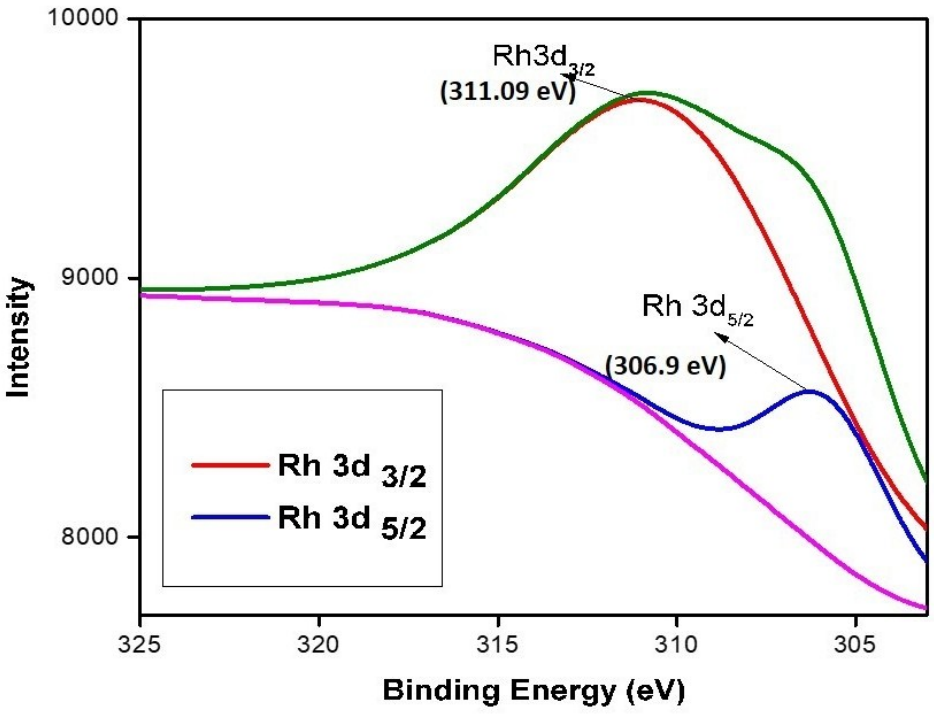

Figure S7: The XPS spectrum of the DMF-protected Rh NC.

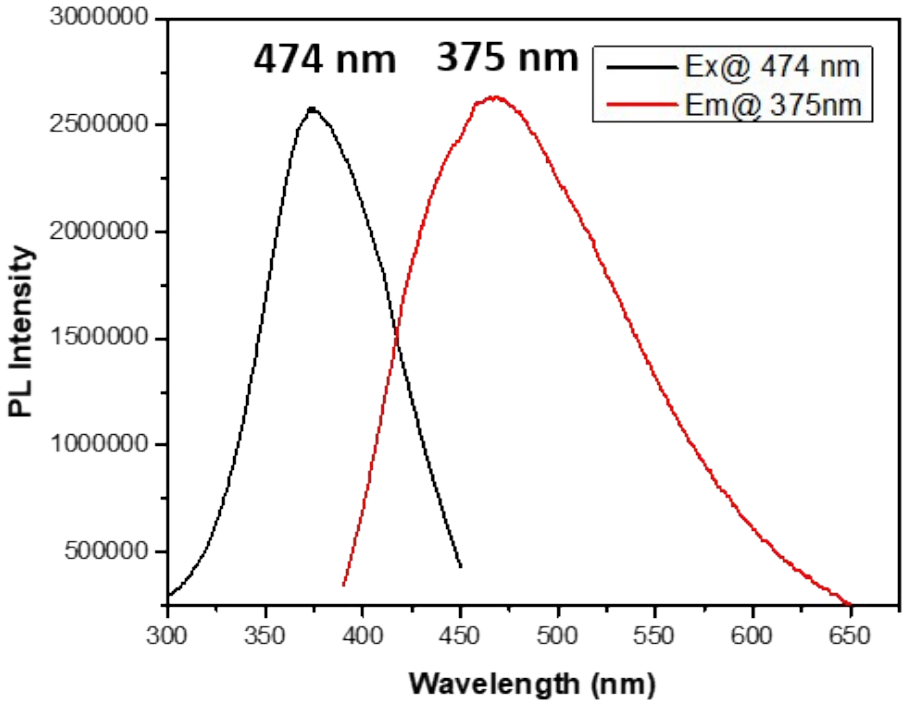

Figure S8: Emission spectra of the Rh NC.

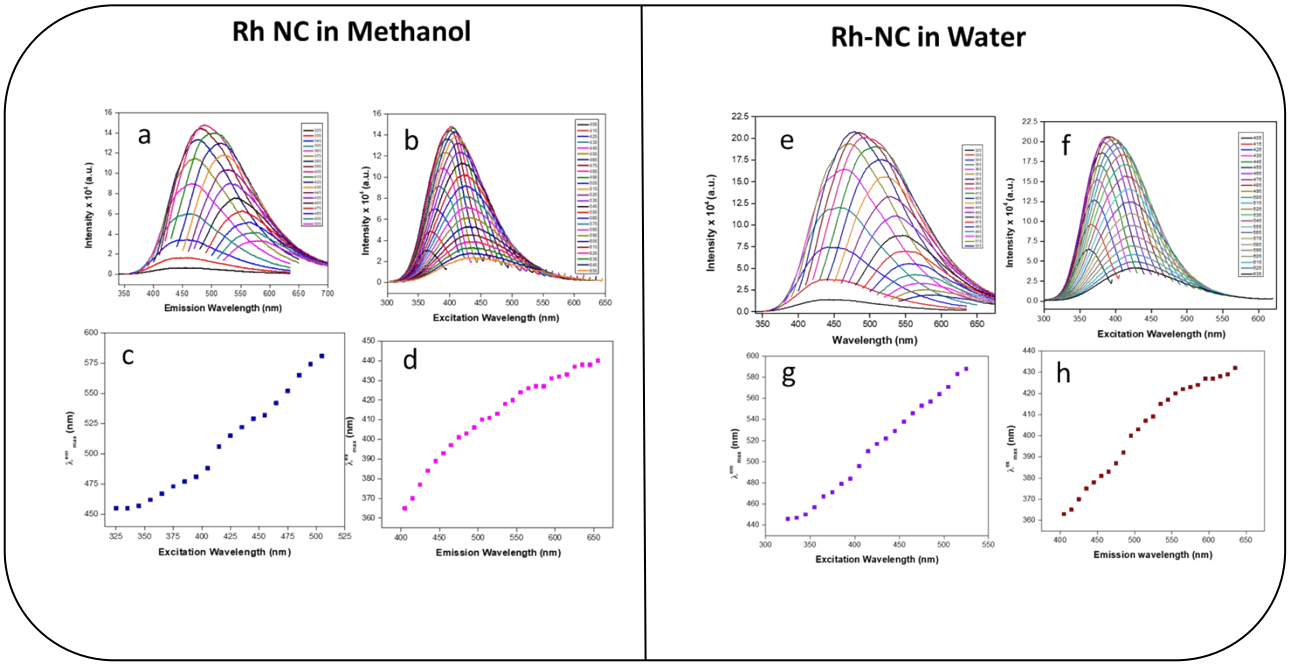

Figure S9. (a) and (e) are the emission spectra at different excitation wavelength. (b) and (f) are excitation spectra at different emission wavelength. (c) and (g) represent the fluorescence maxima (λ_{max}^{em}) as a function of excitation wavelength (λ_{ex}). (d) and (h) represent excitation maxima (λ_{max}^{ex}) as a function of fluorescence wavelength (λ_{em}).

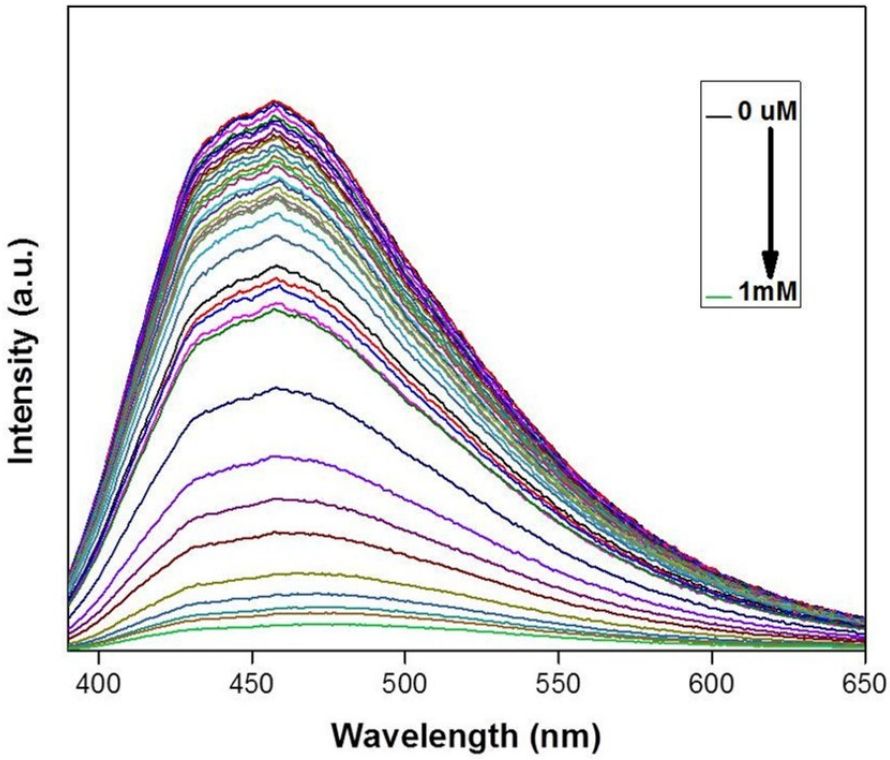

Figure S10. Emission spectra of Rh NC solution in the presence of different Cr(VI) ion concentration.

(a)

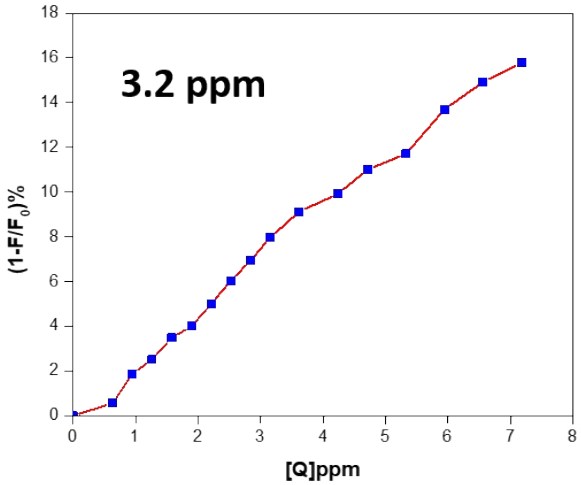

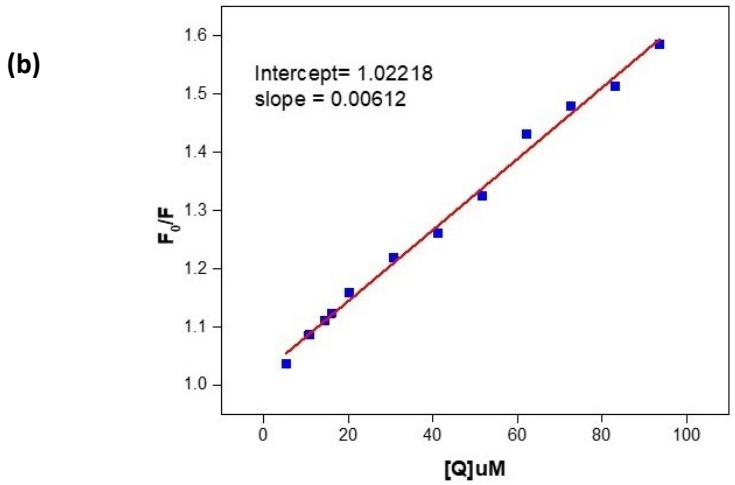

Figure S11. Relative fluorescence of Rh NCs as a function of Cr(VI) ion concentration showing the (a) resulting in a linear Stern-Volmer plot, (b) sensitivity of the Rh NC.

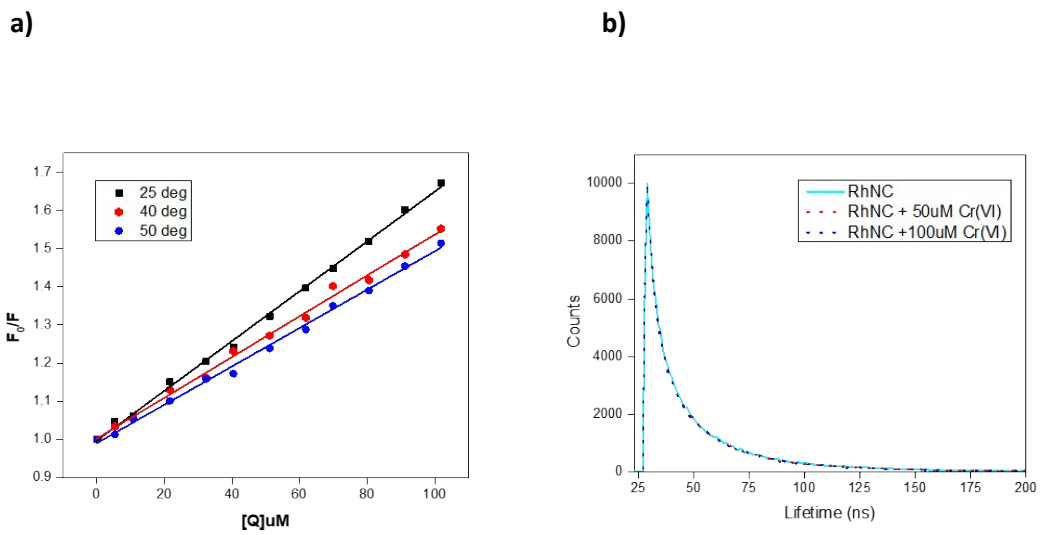

c)

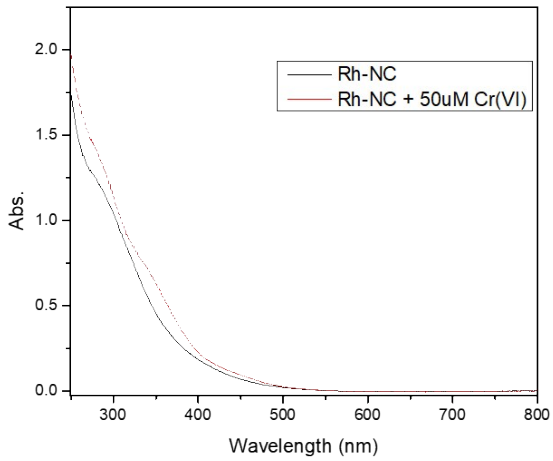

Figure S12. a) Temperature dependent Stern-Volmer plot generated by the addition of different concentration of Cr(VI) ion to the Rh NC. b) Fluorescence decay profile of Rh NC in absence and presence of $Cr_2O_7^{2-}$ ion. c) Absorbance spectra of Rh NC before and after addition of $Cr_2O_7^{2-}$ ion.

Table S1. Temperature dependent Stern-Volmer (K_{sv}) and bimolecular quenching constants (kq) of the Rh NC after addition of $Cr_2O_7^{2-}$ ion.

T/K	K_{sv} (M^{-1})	kq ($M^{-1}.s^{-1}$)

298	6.50×10^3	1.79×10^{12}
313	5.35×10^3	1.47×10^{12}
323	5.03×10^3	1.46×10^{12}

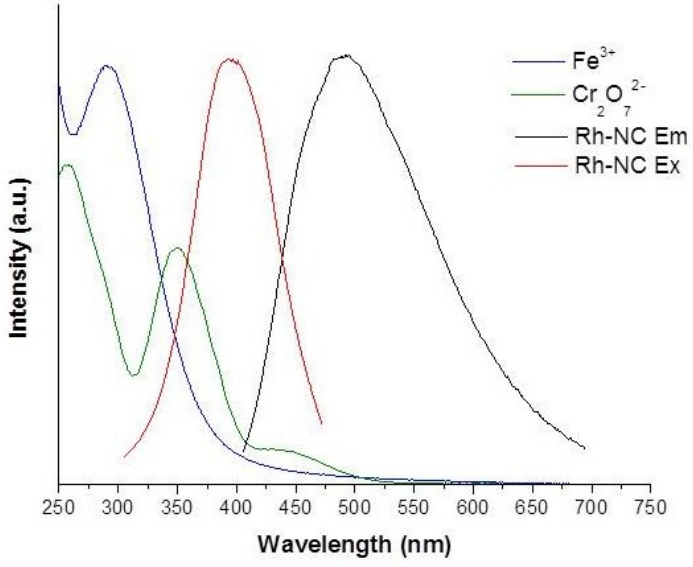

Figure S13. Spectral overlaps between the UV-vis absorption spectrum of $Cr_2O_7^{2-}$, Fe^{3+} and the excitation and emission spectra of Rh NC in water.

Table S2: Comparison of the sensing efficiency of the two cluster having similar optical property.

Methods	**Materials used**	**Linear range/μM**	**LODs/ M**	**Refs.**
Fluorescence	IrNCs	0.1 to 100	0.025×10^{-6}	1
Fluorescence	RhNCs	1 to 100	11×10^{-6}	current
Fluorescence	CuNCs	0.2–60	0.065×10^{-6}	2
Fluorescence	CdTe quantum dots	0.2–20	0.154×10^{-6}	3
Fluorescence	Silicon nanoparticles	0.1–200	0.028×10^{-6}	4
Fluorescence	Carbon dots	1–10	0.2×10^{-6}	5
Fluorescence	Graphene quantum dots	0.05–500	0.0037×10^{-6}	6